SCIENCE CHINA
Physics, Mechanics & Astronomy

• Article •
Special Issue: Physical Mechanics

June 2012 Vol.55 No.6: 989–995
doi: 10.1007/s11433-012-4724-7

Investigating effects of nano-particles infiltration on mechanical properties of cell membrane using atomic force microscopy

ZHANG XiaoYue[1,2], ZHANG Yong[2], ZHENG Yue[1,2*] & WANG Biao[1,2*]

[1] *School of Engineering, Sun Yat-sen University, Guangzhou 510275, China;*
[2] *State Key Laboratory of Optoelectronic Materials and Technologies/Institute of Optoelectronic and Functional Composite Materials, School of Physics and Engineering, Sun Yat-sen University, Guangzhou 510275, China*

Received January 11, 2012; accepted March 16, 2012; published online April 18, 2012

In this paper, we introduce our finding of the effects of C_{60} nanoparticles (NP) infiltration on mechanical properties of cell and its membrane. Atomic force microscopy (AFM) is used to perform indentation on both normal and C_{60} infiltrated red blood cells (RBC) to gain data of mechanical characteristics of the membrane. Our results show that the mechanical properties of human RBC membrane seem to be altered due to the presence of C_{60} NPs. The resistance and ultimate strength of the C_{60} infiltrated RBC membrane significantly decrease. We also explain the mechanism of how C_{60} NPs infiltration changes the mechanical properties of the cell membrane by predicting the structural change of the lipid bilayer caused by the C_{60} infiltration at molecular level and analyze the interactions among molecules in the lipid bilayer. The potential hazards and application of the change in mechanical characteristics of the RBCs membrane are also discussed. Nanotoxicity of C_{60} NPs may be significant for some biological cells.

human red blood cell, mechanical properties, C_{60} nano-particles infiltration, atomic force microscope

PACS number(s): 87.16.Dg, 87.64.Dz, 87.15.La, 87.17.-d

Citation: Zhang X Y, Zhang Y, Zheng Y, et al. Investigating effects of nano-particles infiltration on mechanical properties of cell membrane using atomic force microscopy. Sci China-Phys Mech Astron, 2012, 55: 989–995, doi: 10.1007/s11433-012-4724-7

In recent years, nano-particles (NP) have been proved to possess many potential applications in bio-medicines [1–5]. However, due to their small size, NPs can easily infiltrate living cells thereby altering the molecular structure, and disturbing the functions of the cell [6,7]. This phenomenon is referred to as nanotoxicity. Consequently, with regard to the applications of NPs as biomedicine, the interaction between cell and NPs has become a new topic of considerable scientific interest and medical significance [8–11].

It has been known that mechanical characteristics of the cell membrane significantly influences the biological functions of cells [12,13]. Many direct connections between the progression of certain inherited diseases and the mechanical characteristics of cells have been shown [14]. For example, sickle cell is found to be caused by a defect in the hemoglobin structure of the human red blood cell (RBC). As a consequence of this abnormal hemoglobin, the shape of the RBC is altered and its deformability and biorheology are adversely affected [15]. These influences can result in severe pain as the tissues surrounding the blood vessels receive insufficient oxygen. Other examples such as anisocytosis, hereditary spherocytosis and malaria are also known to affect proper cell function by changing the mechanical properties of the cell [16–18]. Generally speaking, recent researches have indicated that the mechanical information of cell membrane is critical for bio-processes, diseases and toxicity of the cell [19].

The effect of NPs on mechanical characteristics of cells membrane become a focus in recent years. Theoretical mo-

*Corresponding author (ZHENG Yue, email: zhengy35@mail.sysu.edu.cn; WANG Biao, email: wangbiao@mail.sysu.edu.cn)

lecular dynamics (MD) simulations regarding the effect of C_{60} (Fullerene), a hydrophobic spherical molecule composed of 60 carbon atoms and with the diameter of 0.7 nm, on infiltration into the lipids bilayers has been studied. Results have shown that C_{60} NPs have the ability to easily infiltrate into the lipids bilayer, remaining between the lipids, and finally altering the molecular structure and interactions between the lipids [20–23]. It can be inferred that infiltration of C_{60} particles has the ability to affect the function of the cell, and exhibits cytotoxicity on people and animals [24–30]. Currently, the pathogenesis of the toxicity of C_{60} NPs is not yet clear. In the process of C_{60} infiltration, which is very stable chemically [20], the nanotoxicity may not result from the chemical reaction but from the change of the cell membrane mechanical characteristics. Therefore, it is critical to clarify differences of mechanical properties between cell membrane with and without C_{60} infiltration, respectively.

In this paper, we investigate the mechanical characteristics of the RBC membrane with and without C_{60} NPs (Figure 1), respectively, and comprehensively discuss the effect of the C_{60} NPs on the mechanical characteristics of the RBC membrane by interrupting the molecular structure of phospholipids bilayers. Atomic force microscopy (AFM) is used to perform indentation on both normal and C_{60} infiltrated RBCs to gain data of the mechanical characteristics of the RBC membrane. The data from these experiments show that the resistance and ultimate strength of the RBC membrane both decrease with C_{60} infiltration, which implies that the mechanical properties seem to be altered due to effect of C_{60} infiltration. The mechanism of how C_{60} NPs infiltration changes the mechanical properties of the cell membrane is also discussed in this paper. By predicting the structural change of lipids bilayers caused by infiltration of C_{60} at molecular level and analyzing the interactions among molecules, we give an explanation of this observation. The potential hazards and applications of the changes in stress-strain relation of cell membrane caused by C_{60} infiltration are also discussed.

1 AFM indentation on both RBCs with and without C_{60} presence

1.1 Sample preparation

To investigate the mechanical properties of cell with and without C_{60} presence, we use human RBC and its membrane as sample. RBC has a relatively simple structure and readily facilitates single cell mechanical deformation experiments [18,29,30]. Human RBCs were separated from blood of a healthy donor using centrifugation. Two groups of samples were prepared, which were normal RBCs and those RBCs with C_{60} infiltration (Figure 1). The normal RBCs sample can be simply obtained by adding 1.5 mL pure RBCs to

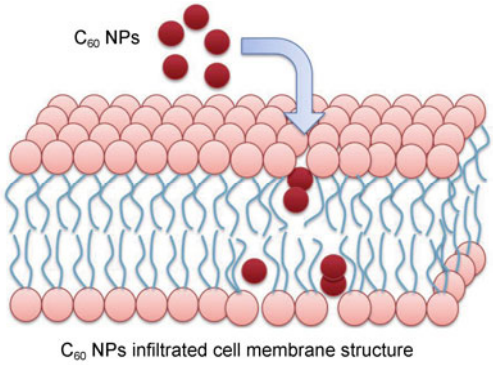

Figure 1 (Color online) Illumination of normal and the C_{60} infiltrated lipid bilayer. After the C_{60} NPs enter the phospholipid bilayer, instead of the central plane of the membrane, it is most probably below the head groups. If concentration of C_{60} is large enough, the nanoparticles may assemble together and become clusters.

1.5 mL Alsever's solution. To prepare the sample of the RBCs with presence of C_{60}, 50 mg C_{60} NPs were first added to 10 mL Alsever's Solution. The mixture was placed in a ultrasonic cleaning machine for 25 min to disperse the C_{60} NPs. We then kept the mixture still for 5 min. Because of their hydrophobicity, C_{60} NPs tend to gather in clusters and the C_{60} clusters tend to go down to the bottom of the cuvette because of gravity. Therefore it can be seen that the upper part of the mixture was limpid. We adopted the supernatant as the C_{60}-added Alsever's solution, in which the C_{60} NPs were dispersed uniformly. Then 1.5 mL RBCs were quickly added into 1.5 mL C_{60}-added Alsever's solution before the C_{60} NPs were gathered. After that, the sample mixture was kept still under room temperature for 20 min, thus allowing the C_{60} NPs to infiltrate the RBCs membrane. The RBCs sample with C_{60} NPs presence was also prepared. The mixtures of RBCs with and without C_{60} NPs were then put on silicon substrate, respectively. Using spin coating method, a single layer of RBCs were dispersed uniformly on the Si substrate. It should be noted that although the concentration of the C_{60} NPs is high in the process of preparing RBCs with C_{60} NPs presence, not all the C_{60} NPs actually penetrated the cell membrane. Considering that the AFM tip only contacts the cell membrane in a concentrated area, a high concentration of C_{60} NPs in the mixture is required.

1.2 AFM indentation

The AFM [31] has emerged from an imaging device to a force sensing device at the nanometer and piconewton scale. For its ability to apply a local force up to 100 nN, the AFM has been widely used in biomechanics research [32–35]. AFM provides the method to apply a local deformation on the cell membrane, which allows researchers to analyze the mechanical properties of the lipid bilayer. A schematic diagram of the AFM indentation is shown in Figure 2. To perform the AFM indentation, CSPM5500 Scanning Probe Microscope System (Being Nano-Instruments, Ltd.,) was

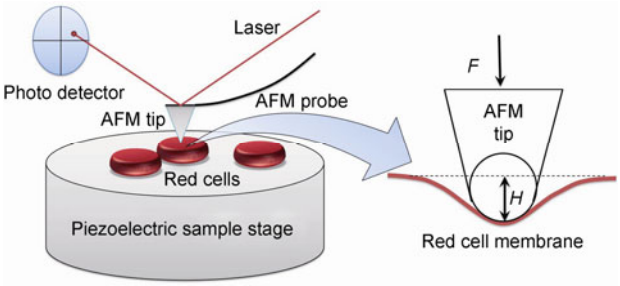

Figure 2 (Color online) The sketch map of AFM indentation. Single layer of RBCs were placed on the piezoelectric stage. With the rise of piezoelectric stage, the force can be applied on the RBC by the tip. The value of the force can be measured by recording the deflection signal of the cantilever using a laser and photo detector.

used in our experiment. A single layer of RBCs without or with C_{60} infiltration were placed on the piezoelectric sample stage (Figure 3), respectively, which has a piezoelectric coefficient of 17 nm/V. With the rise of the sample stage, the RBCs contact the probe with the force constant of which is 0.02 N/m, The curvature radius of the tip is 20 nm. By recording the deflection signal of the cantilever and the piezoelectric signal, the images of the sample can be obtained. When performing the indentation, the tip approached and pressed the RBCs samples with a speed of 20 nm/s or 2000 nm/s and generated a local deformation on the cell surface. The resulting deflection of the cantilever tip can be calibrated to estimate the applied force, which can then provide a high resolution image of the mechanical properties. It is possible to extract information regarding the elasticity of the cell by studying the indentation curves [36,37].

1.3 Results

The RBCs samples with and without C_{60} infiltration were imaged by AFM, which are shown in Figures 3(a) and 3(b), respectively. The biconcave disc shape of RBC can be seen clearly. Among the RBCs is the substrate, which shows that there was only one layer of RBCs on the substrate in our experiments. In the comparison between images of RBCs with and without C_{60}, no difference in morphology was observed. In AFM indentation, more than 200 samples were tested, and the curves of tip indentation depth H and the applied force F (Figure 4) on the membrane by the tip of them were measured. We also performed fast indentation to invest the ultimate strength of the RBC membrane with and without C_{60} infiltration. In fast indentation, the downward speed of AFM tip is 2000 nm/s, which is one hundred times faster than the ordinary AFM indentation.

From the experiments results of the AFM indentation, two important observations can be seen. The first observation can be seen in Figure 4, which shows several examples of the Force-indentation depth curves (*F-H* curves) of normal (circle-lines) and C_{60} infiltrated (square-lines) RBCs measured by AFM indentation. The *F-H* curves reflect the resistance of the sample to the tip. Under the same value of force, the larger indentation depth can be interpreted that the sample is less resistant to the indentation, thus the sample is considered to be softer. It can be seen that the slope of the *F-H* curves of RBCs with C_{60} is smaller than that of the normal the RBCs, therefore the indentation depth H of C60 infiltrated RBC is larger than that of normal the RBC under the same value of force. This implies that the RBCs with C_{60} presence is softer than the normal RBCs. It can also be seen that the distribution of the indentation curves of C_{60} infiltrated samples is not as concentrated as that of the normal RBCs. This reflects the fact that the extent of change of the mechanical properties is related to the concentration of C_{60} NPs that enter the membrane. The other observation is seen in the fast indentation that RBC membrane in the presence of C_{60} NPs which can be pierced easily by the tip. As pointed out in Figure 5, inflection can be found in *F-H* curves of C_{60} infiltrated samples, implying that the samples were pierced. This phenomenon can only be found in C_{60} infiltrated cell membrane, which shows that the presence of C_{60} is able to weaken the cell membrane and make more readily to be pierced. The results from the AFM indentation

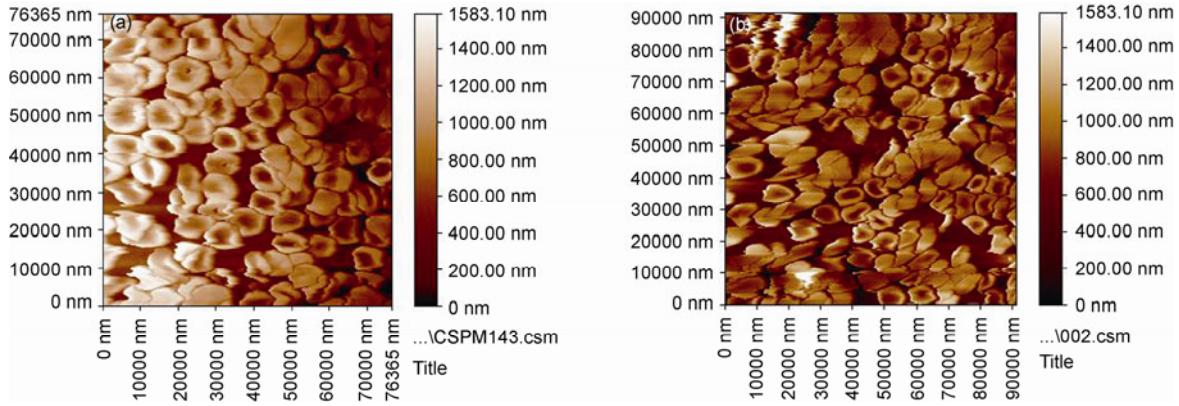

Figure 3 (Color online) (a) Normal RBCs samples imaged by AFM in the contact model. The biconcave shape of RBC can be clearly seen. Among the RBCs is the flat substrate, which shows that there was only one layer of RBCs on the substrate. (b) Image of RBCs with C_{60} infiltration.

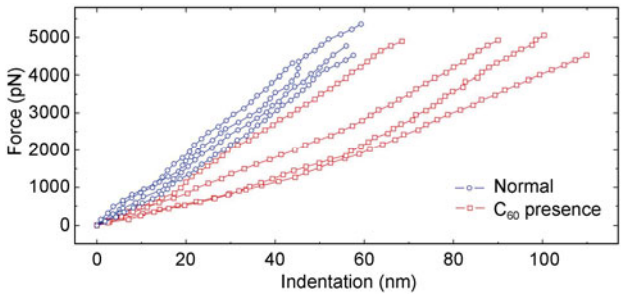

Figure 4 (Color online) *F-H* curves of both normal and C_{60} infiltrated RBC. The slope of the *F-H* curves of samples with C_{60} is smaller than that of the normal one, thus the indentation depth *H* of C_{60} infiltrated RBC is larger than that of the normal RBC under the same value of force. The RBCs with C_{60} presence are softer than for normal RBCs.

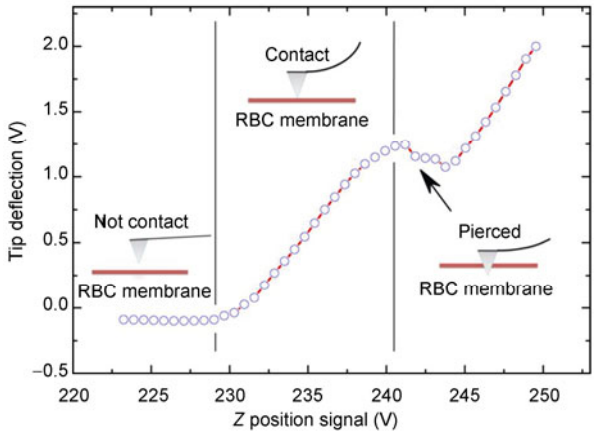

Figure 5 (Color online) Examples of *F-H* curves，which show that the sample RBC is pierced.

is direct evidences that C_{60} NPs have the ability to change the mechanical characteristics of the RBC membrane. The effect of change in mechanical properties on the function of RBCs will be discussed later in this paper.

2 The mechanism of how C_{60} NPs change the mechanical characteristics of RBC membrane

To explain how C_{60} NPs change the mechanical characteristics of RBC membrane, we shall first investigate the changes in molecular structure caused by C_{60} infiltration. Recent MD simulation studies [20] report that the process of C_{60} NP can infiltrate into the lipid bilayer. It is observed that the C_{60} molecule initially diffuses slowly toward the bilayer initially. However, in a few nanoseconds, the C_{60} molecule virtually infiltrates into the lipid bilayer and then remains in the lipid bilayer for the remainder of the simulation. After the C_{60} molecule has entered the lipids bilayers, instead of the central plane of the membrane, its most probable the *z*-position which is z=1 nm, very close to the boundaries z=±1.5 nm. This can be seen below the head group (Figure 1). If there are several C_{60} molecules enter the lipids bilayers, the C_{60} NPs might assemble to be a cluster at the *z*-equilibrium position. Due to the presence of C_{60} NPs, the relative positions of lipids are affected, which could signal that the molecular structure of lipid bilayer is altered.

It can be easily inferred that change in molecular structure will certainly change the interaction between molecules of the lipids bilayers. The interaction between two adjacent lipids and interactions between C_{60} NP and the lipids in proximity to it are defined to be short range interaction. Long range interactions are referring to the interactions between two nonadjacent molecules. For simplicity, in the analysis of the molecular interactions, we assume that long range interaction can be ignored and only short range interaction be considered. This simplification is acceptable for two reasons. First, the short range interactions comprise the main part of the total elastic potential of the lipids bilayers. Moreover, the contact area between AFM tip and the RBC membrane is insignificant in contrast to the whole cell, and C_{60} NPs can be assumed to distribute uniformly in the lipid bilayer. Thus, non-local effect, in which the long range interactions are crucial, can be not considered. Therefore, ignoring the long range interaction dose not seriously affect the analysis. The physical pictures of interactions of two lipid molecules with and without C_{60} NPs presence are shown in Figure 6, in which a lipid is simplified to consist of a head group and tail group. In the *z*-direction, the equilibrium position of the C_{60} NP in the lipids bilayers is the result of the competition between the energy cost to vacate the space to be occupied by the C_{60} NPs and the energy gained due to the interactions between the infiltrated C_{60} molecule and its surroundings [20]. It can be implied that both head group and tail group apply a repulsive force on the C_{60} NP in lipids bilayers, which is shown in Figure 6. The head groups repulse the C_{60} NP by hydrophobic interaction. Because the tail groups tend to resist the C_{60} NP from occupying the space between them, the interaction between tail group and C_{60} NP also tend to be repulsed. To describe the interaction between molecules in lipids bilayers qualitatively, we simply apply Lennard-Jones-like potential in the analysis [38], which is shown in Figure 7. The interaction between lipids in normal membrane is shown by the red line. It can be seen that the maximum force between lipids is the highest and the slope of the curve is largest, implying that the interaction between lipids in normal cell membrane is strong. The interaction between C_{60} NP and the lipids can be given as the green line in Figure 7. As discussed before, C_{60} NP tend to be repulsive to the lipids thus the curve showing that the force between C_{60} NP and lipids tend to push each other away in a longer distance. By combining the two potentials, the equivalent potential of two lipids with C_{60} presence can be obtain, which is shown by the blue line. Three obvious changes can be viewed in the comparison between the blue line and red line. The maximum force of the interaction between lipids is weakened, which is

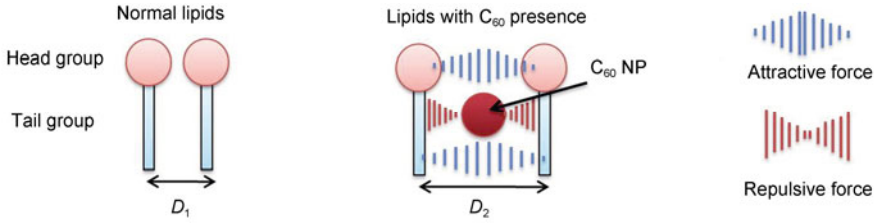

Figure 6 Schematic illustration of normal and C_{60} infiltrated lipids and the interactions between lipids and C_{60} NP. Without the presence of C_{60}, the interactions between the lipids result in lipids staying in equilibrium distant of each other. If there is a C_{60} cluster between the two lipids, it will be repulsive to both head and tail group. Resistance by the repulsive force, the head group and tail group tend to attract the head group and tail group of the other lipids, respectively. The equilibrium distant of each lipids is thus changed.

shown in Figure 7 as Δf. The slope of the curve of equivalent potential of two lipids with C_{60} presence is smaller than that of the normal one, which implies that the interaction between two lipids is softened. Also, the relative equilibrium distance of the two lipids near the infiltrated C_{60} NP is enlarged by ΔD due to the repulsive interaction between C_{60} NP and the lipid. To explain this observation, we can consider the interaction between the lipid as elastic bonds, which is shown in Figure 8. Before indentation, the bonds between the lipid is unstretched (Figure 8(a)), and the distant between the lipid is equal to the equilibrium distance. When the tip is pressed on the RBC membrane, the bonds are stretched to provide the resistance to the tip, which is shown in Figure 8(b). Because the bonds between lipids of the C_{60} infiltrate RBCs membrane is softer than that of the normal one, under the same force applied by the tip, the distant between two lipids with a softer bond becomes longer. Therefore, the indentation depth of C_{60} infiltrated RBCs membrane is larger than that of the normal one. With the presence of C_{60} NP, the maximum bond force between the lipids decrease. Thus with the tip pressed harder, the bonds in C_{60} NP infiltrated lipids bilayers reaching their maximum force more rapidly than the normal one (Figure 8(c)), which cause the membrane to easily pierced by the

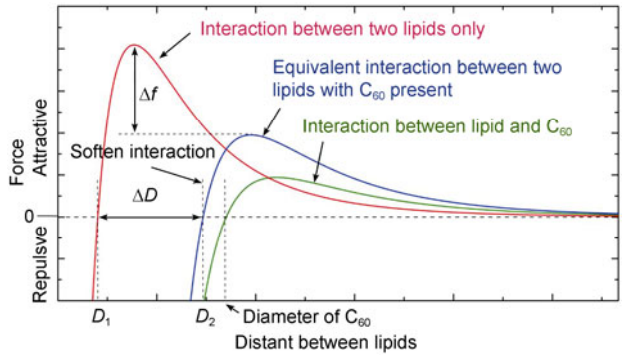

Figure 7 Schematic illustration of normal and C_{60} infiltrated lipids and potential between lipids and C_{60} NPs. Without the presence of C_{60}, the potential between lipids can be described by the red line. If there is a C_{60} NP between the two lipids, it will interact with both the head and tail groups and form the green line. Therefore, the effect of green line should be pulsed with the red line to form the effective potential between the two lipids, which is shown as the blue line.

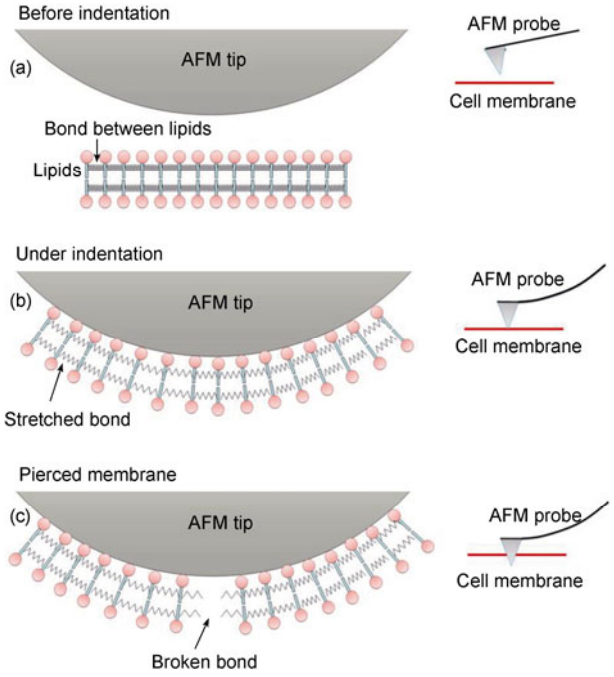

Figure 8 Schematic illustration of the interaction between lipids under AFM indentation. The interaction between lipids is shown as elastic bonds. (a) Before the tip contact with the lipids bilayers, the bond is unstretched; (b) the bonds stretched to resist the force applied by the tip; (c) with the tip pressed harder, the bonds between lipids might fail to resist the force and be broken.

AFM tip. The change in relative equilibrium distance also contributes to the easily pierced RBC membrane. The longer distance between the lipid molecules may result in fewer lipids contacting with the tip, therefore, there are fewer bonds to store the energy caused by the deformation of the membrane. This can be interpreted that when the tip had done the same amount of work to the membrane in indention, the energy of each bonds in C_{60} infiltrated RBC membrane is more than that in the normal membrane. This may explain why the RBC membrane with C_{60} presence is easily pierced by the AFM tip.

3 Discussion and conclusion

The softening of the RBC membrane implies that it may be

risky to apply NPs in medical treatment using mass dosages [39]. The effect of mass dosages of C_{60} NPs on the RBC membrane may be like malaria, a disease resulting from the merozoites which changes and destroys the molecular structure of RBCs membrane and causes fever and disseminated intravascular coagulation (DIC). This result also implies that the ultimate strength of the cell membrane is reduced by C_{60} NPs. The ultimate strength corresponds to the largest force the membrane that can provide resistance to an applied load. It can be seen in our experiment that the ultimate stress of the cell is reduced due to the infiltration of C_{60} NPs. RBCs confront different forces in blood circulation. If their ultimate strength decreases, many of them would dehisce in the circulation. In this case, hemolytic anemia could occur, the consequence being serious and possibly fatal. Not limited to RBCs, most cells of humans have a similar membrane structure, therefore, C_{60} also has the ability to change their mechanical characteristics and cause different effects on their functions. For example, our results provide the explanation for the experimental results as reported by Sayes et al. [28] that human skin (HDF) and liver carcinoma (HepG2) cells begin to exhibit signs of leaky membranes after 30 hours of exposure to C_{60} NPs.

Although there are potential risks in the medical application of C_{60} NPs, it should be noted that the ability of C_{60} NPs to change mechanical characteristics of cell membrane might also be valuable for therapies of certain diseases. For examples, mechanical properties of cell membrane are essential for the function of bacteria. By changing the mechanical properties of cell membrane, C_{60} NPs might provide an alternative method to kill the bacteria that are harmful to human health, while the traditional antibiotics result in drug resistance of these bacteria. Another possible medical application might be using C_{60} NPs to regulate the mechanical properties of cells that are already sick or deteriorating due to aging. An appropriate amount of C_{60} NPs may aid or maintain the mechanical properties and functions of the cells in these situations. So far, little work has been devoted on utilizing the ability of C_{60} NPs to change mechanical characteristics of cell membrane, and further research is needed.

To summary, we have investigated how the mechanical characteristics of human RBCs membrane are altered by C_{60} NPs infiltration based on experimental methodology and theoretical analysis. The results performed by the AFM indicate that the mechanical properties of human RBC membrane were altered due to the presence of C_{60} NPs, the resistance and ultimate strength of the C_{60} infiltrated RBC membrane were both significantly decreased. To explain this observation, a simple model based on molecular interaction was developed. In this model, structural change of the lipid bilayer caused by the infiltration of C_{60} was discussed at the molecular level and the interactions among the molecules were analyzed. The theoretical analysis explains the experiment data, which are consistent to the mechanical properties that the RBC membrane are changed by C_{60} NPs infiltration. We believe that the infiltration of C_{60} NPs will make the cell membrane softer and more susceptible to breakage. Our results may provide an important reference to the safe application of C_{60} NPs and to the development of new therapies using NPs in bio-medical engineering.

This work was supported by the National Natural Science Foundation of China (Grant Nos. 10902128, 11072271, 10972239, 51172291), Fundamental Research Funds for the Central Universities, New Century Excellent Talents in University and Research Funds for the Doctoral Program of Higher Education.

1 Salata OV. Applications of nanoparticles in biology and medicine. J Nanobiotech, 2004, 2: 3–8
2 Panyam J, Labhasetwar V. Biodegradable nanoparticles for drug and gene delivery to cells and tissue. Ad Drug Delivery Rev, 2003, 55, 329–347
3 Mark E D, Zhou C, Dong M S. Nanoparticle therapeutics: an emerging treatment modality for cancer. Nat Rev-Drug Dis, 2008, 7: 711–782
4 David A G, Dwight S S, Westton L D, et al. Gold nanoparticles for biology and medicine. Angew Chem Int Ed, 2010, 49: 3280–3294
5 Shashi K M. Nanoparticles in modern medicine: State of the art and future challenges. Inter J Nanomed, 2007, 2(2): 129–141
6 Fischer H C, Chan W CW. Nanotoxicity: the growing need for in vivo study. Current Opinion Biotech, 2007, 18: 565–571
7 Chithrani B D, Ghazani A A, Chan W CW. Determining the size and shape dependence of gold nanoparticle uptake into mammalian cells. Nano Lett, 2006, 6(4): 662–668
8 Medina C, Santos-Martinez M J, Radomski A, et al. Nanoparticles: Pharmacological and toxicological significance. British J Pharm, 2007, 150: 552–558
9 Virender K S. Aggregation and toxicity of titanium dioxide nanoparticles in aquatic environment-A review. J Enviro Sci Health Part A, 2009, 44: 1485–1495
10 Li S Q, Zhu R R, Zhu H, et al. Nanotoxicity of TiO2 nanoparticles to erythrocyte in vitro. Food Chem Toxicol, 2008, 46: 3626–3631
11 Jin Y H, Kannan S, Wu M, et al. Toxicity of luminescent silica nanoparticles to living cells. Chem Res Toxicol, 2007, 20: 1126–1133
12 Tobias B, Benjamin R C, Chen Z, et al. Thermodynamics and mechanics of membrane curvature generation and sensing by proteins and lipids. Annu Rev Phys Chem, 2011, 62: 483–506
13 SURESH S. Mechanical response of human red blood cells in health and disease: Some structure-property-function relationships. J Mater Res, 2006, 21(8): 1871–1877
14 Mohandas N, Evans E A. Mechanical properties of the red cell membrane in relation to molecular structure and genetic defects. Annu Rev Biophys Biomol Struct, 1994, 23: 787–818
15 Platt O S. The sickle syndrome. Haldin R I, Lux S E, Stossel T P, eds. Blood: Principles and Practice of Hematology. Philadelphia: J. B. Lippincott, 1995. 1592–1700
16 Cooke B M, Mohandas N, Coppel R L. The malaria-infected red blood cell: Structuraland functional changes. Adv Parasitol, 2001, 50: 1–86
17 Glenister F K, Coppel R L, Cowman A F, et al. Contribution of parasite proteins to altered mechanical properties of malaria-infected red blood cells. Blood, 2002, 99(3): 1060–1063
18 Lim C T, Dao M, Suresh S, et al. Large deformation of living cells using laser traps. Acta Mater, 2004, 52: 1837–1845
19 Lulevich V, Zimmer C C, Hong H S, et al. Single-cell mechanics

provides a sensitive and quantitative means for probing amyloid-β peptide and neuronal cell interactions. PNAS, 2010, 107(31): 13872–13877
20 Qiao R. Translocation of C60 and its derivatives across a lipid bilayer. Nano Lett, 2007, 7(3): 614–619
21 Li L, Davande H, Bedrov D, et al. A molecular dynamics simulation study of C60 fullerenes inside a dimyristoylphosphatidylcholine lipid bilayer. J Phys Chem B, 2007, 111: 4067–4072
22 Jirasak W E, Svetlana B A, Wannapong T, et al. Computer simulation study of fullerene translocation through lipid membranes. Nat Nanotech, 2008, 3: 363–368
23 Chang R, Lee J. Dynamics of C60 molecules in biological membranes: Computer simulation studies. Bull Korean Chem Soc, 2010, 31(11): 3195–3200
24 Powell M C, Kanarek M S. Nanomaterial health effects—part 2: Uncertainties and recommendations for the future. Wisconsin Med J, 2006, 105(2): 16–20
25 Motohiro U O, Tsukasa A, Fumio W, et al. Toxicity evaluations of various carbon nanomaterials. Dental Mater J, 2011, 30(3): 245–263
26 Zhu X, Zhu L, Li Y, et al. Developmental toxicity in Zebrafish (Danio Rerio) embryos after exposure to manufactured nanomaterials: Buckminsterfullerene aggregates (nC60) and fullerol. Enviro Toxicol Chem, 2007, 26: 976–979
27 Oberdörster E. Manufactured nanomaterials (Fullerenes, C60) induce oxidative stress in the brain of Juvenile largemouth bass. Enviro Health Perspect, 2004, 112: 1058–1062
28 Sayes C M, Fortnerz J D, Guo W, et al. The differential cytotoxicity of water-soluble fullerenes. Nano Lett, 2004, 4(10): 1881–1887
29 Sen S, Subramanian S, Discher D E. Indentation and adhesive probing of a cell membrane with AFM: Theoretical model and experiments. Biophys J, 2005, 89(5): 3203–3213
30 Dao M, Lim C T, Suresh S. Deformation and failure of protein materials in physiologically extreme conditions and disease. J Mech Phys Solids, 2003, 51: 2259–2280
31 Binnig G, Gerber CH, Stoll E, et al. Atomic resolution with atomic force microscope. Surf Sci, 1987, 189-190: 1–6
32 Kuznetsova T G, Starodubtseva M N, Yegorenkov N I, et al. Atomic force microscopy probing of cell elasticity. Micron, 2007, 38: 824–833
33 Scheffer L, Bitler A. Atomic force pulling: Probing the local elasticity of the cell membrane. Eur Biophys J, 2001, 30: 83–90
34 Dimitriadis E K, Horkay F, Maresca J, et al. Determination of elastic moduli of thin layers of soft material using the atomic force microscope. Bio Phys J, 2002, 82: 2798–2810
35 Mathur A B, Collinsworta A M, Reichert W M, et al. Endothelial, cardiac muscle and skeletal muscle exhibit different viscous and elastic properties as determined by atomic force microscopy. J Biomech, 2001, 34: 1545–1553
36 CSPM 5500 SPM User's Manual
37 Vinckier A, Semenza G. Measuring elasticity of biological materials by atomic force microscopy. FEBS Lett, 1998, 430: 12–16
38 Rapaport D C. The Art of Molecular Dynamics Simulation. Cambridge: Cambridge University Press, 2004. 12–13
39 Yeagle P L. Lipid regulation of cell membrane structure and function. FASEB J, 1989, 3: 1833–1842